Supporting Information for:
Quantum scattering pathway of the cofactorless spin-forbidden O_2 addition to DPA-CoA

Javier Hernández-Rodríguez,[a] Susana Gómez-Carrasco*,[a], Cristina Sanz-Sanz,[b] Pablo G. Jambrina[a]

May 26, 2026

[a] Departamento de Química-Física, Universidad de Salamanca, 37008, Spain
[b] Departamento de Química Física Aplicada, Universidad Autónoma de Madrid, Madrid, 28049, Spain

Contents

S1 Potential energy cuts

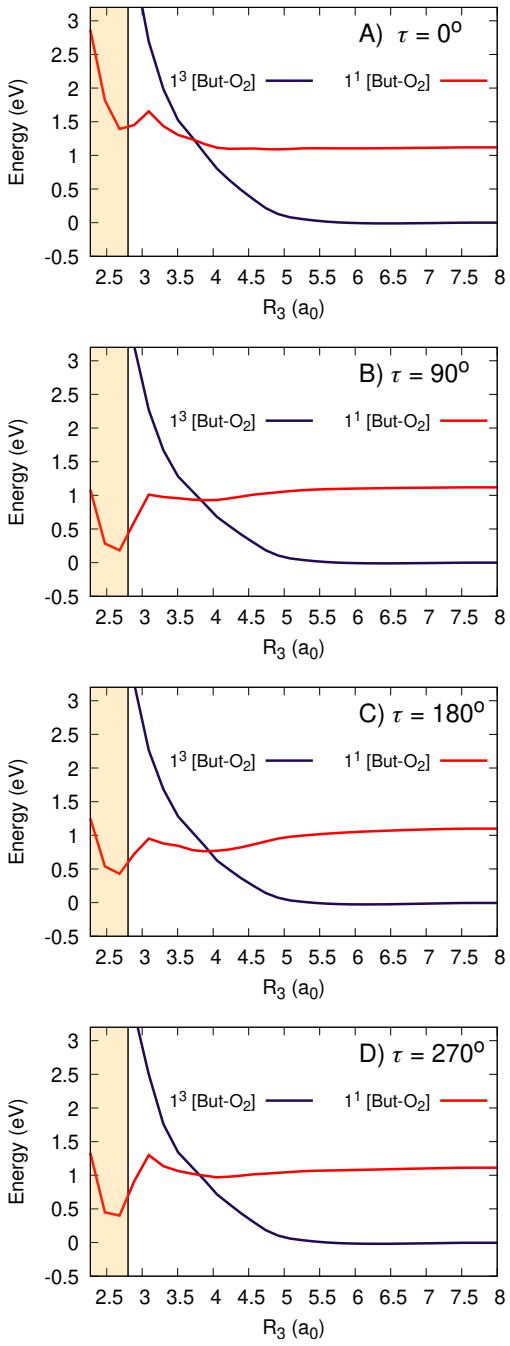

Figure S1 Potential energy cuts of the triplet state, 1^3[But-O_2], and the lowest singlet state, 1^1[But-O_2], for four given torsion angles τ. Coloured area corresponds with the location where the reactive CAP for the formation of the peroxide is located.
Alt Text: Potential energy cuts at four torsional angles τ, showing CAP location.

S2 CAP construction

Quantum dynamical calculations operate on finite grids; when the wavepacket reaches the grid boundary it suffers spurious reflection or transmission artefacts. Complex absorbing potentials (CAPs) eliminate these artefacts by adding a negative imaginary term to the Hamiltonian,[1, 2, 3]

$$-i\eta W(r) = -i\eta (r - r_c)^n \, \theta(r - r_c) \tag{1}$$

where η is the CAP strength, n its order, r_c the onset position, and $\theta(r - r_c)$ the Heaviside step function. r denotes the coordinate along which the CAP is applied, here R_3. A excessively strong CAP introduces spurious reflection, while an insufficiently absorbing CAP allows the wavepacket to reappear at the opposite grid edge. The parameters η, n, and r_c are optimised using the PLCAP functionality implemented in the QUANTICS package,[3] which determines the optimal CAP strength at a fixed length over a given energy range to minimise both reflection and transmission.

The norm loss due to the CAP is directly related to the reactive flux entering the absorbing region. The energy-resolved reaction probability is obtained from the Fourier transform of the wavepacket correlation function [4, 5, 6],

$$P(E) = \frac{2}{|\Delta(E)|^2} \, \mathrm{Re} \int_0^\infty g(\tau) \, e^{iE\tau} \, \mathrm{d}\tau, \tag{2}$$

where $g(\tau) = \int_0^\infty \langle \Psi(t) \, | \, \eta W \, | \, \Psi(t+\tau) \rangle \, \mathrm{d}t$ and $\Delta(E)$ is the energy distribution of the initial wavepacket, and Re denotes the real part of the integral.

Here, two CAPs were employed, with $n = 3$ in both cases. The first was placed at $r_c = 17.50$ a$_0$ with a length of $\Delta r = 2.30$ a$_0$ and strength $\eta = 3.13 \times 10^{-3}$ a.u., absorbing outgoing flux corresponding to the elastic or singlet oxygen formation channel, denoted as CAP ($O_2(X^3\Sigma_g^- \ / \ a^1\Delta_g)$) in Table I of the main text. The CAP for the peroxide formation was placed at $r_c = 2.80$ a$_0$ with $\Delta r = 0.53$ a$_0$ and $\eta = 0.727$ a.u. The position of this CAP required careful optimisation: it must be located sufficiently far from the barrier to avoid premature flux absorption, without compromising the absorbing length or requiring an excessive CAP strength. With $\Delta r = 0.53$ a$_0$, both artefacts remained below 0.1%; convergence tests showed that shorter positions ($r_c = 2.60$–2.70 a$_0$) required higher CAP strengths, whereas positions approaching $r_c = 3.00$ a$_0$ yielded an artificial enhancement of the reaction probability.

S3 Wavepacket evolution

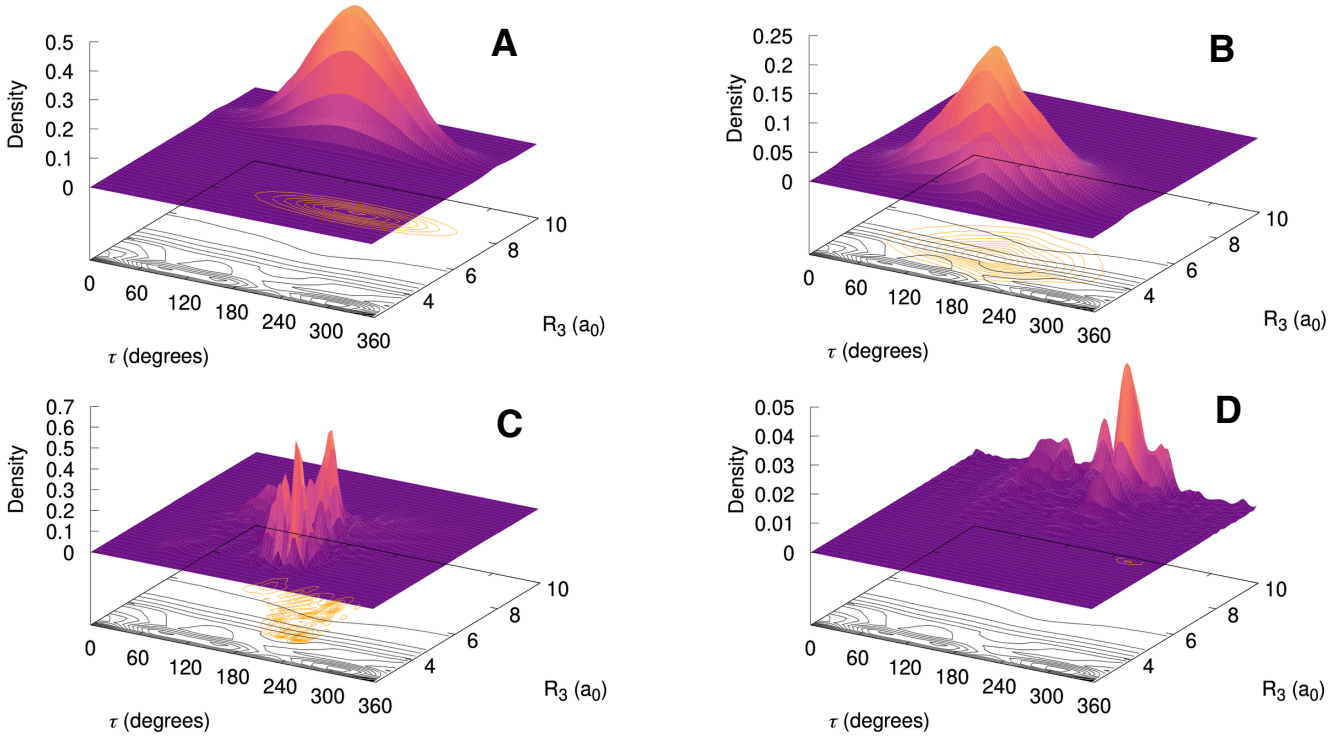

Figure S2 Reduced density of the 2D wavepacket for the LSOD approach at different propagation times: A) 20fs. B) 60fs. C) 120fs. D) 200fs.
Alt Text: Time-resolved 2D wavepacket snapshots (20, 60, 120, 200 fs) for the LSOD propagation.

S4 1S1T probabilities

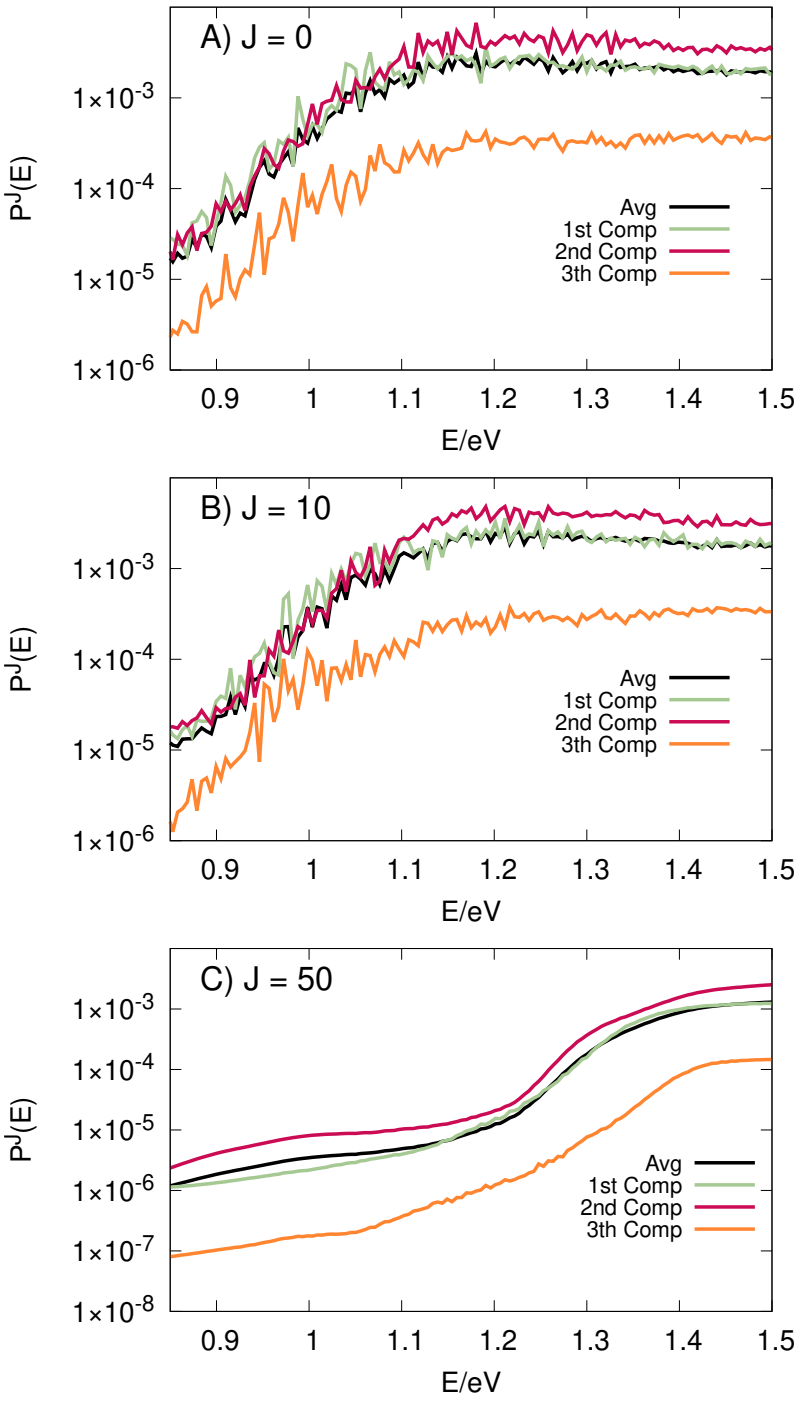

Figure S3 Reaction probabilities as a function of the Energy (in eV) for the formation of the peroxide for J=0, 10 and 50 without starting from the three components of the triplet state, and averaging between them.
Alt Text: Comparison of the individual triplet-component reaction probabilities and their average, for J = 0, 10, 50.

References

[1] Claude Leforestier and Robert E. Wyatt. Optical potential for laser induced dissociation. *J. Chem. Phys.*, 78(5):2334–2344, 1983.

[2] R Kosloff and D Kosloff. Absorbing boundaries for wave propagation problems. *J. Comput. Phys.*, 63(2):363–376, 1986.

[3] M. H. Beck, A. Jäckle, G. A. Worth, and H. D. Meyer. The multiconfiguration time-dependent Hartree (MCTDH) method: A highly efficient algorithm for propagating wavepackets. *Phys. Rep.*, 324(1):1–105, 2000.

[4] Tamar Seideman and William H Miller. Calculation of the cumulative reaction probability via a discrete variable representation with absorbing boundary conditions. *J. Chem. Phys.*, 96(6):4412–4422, 1992.

[5] A Jäckle and H-D Meyer. Time-dependent calculation of reactive flux employing complex absorbing potentials: General aspects and application within the multiconfiguration time-dependent hartree wave approach. *J. Chem. Phys.*, 105(16):6778–6786, 1996.

[6] J Gonzalo Muga, JP Palao, B Navarro, and IL Egusquiza. Complex absorbing potentials. *Phys. Rep.*, 395(6):357–426, 2004.